

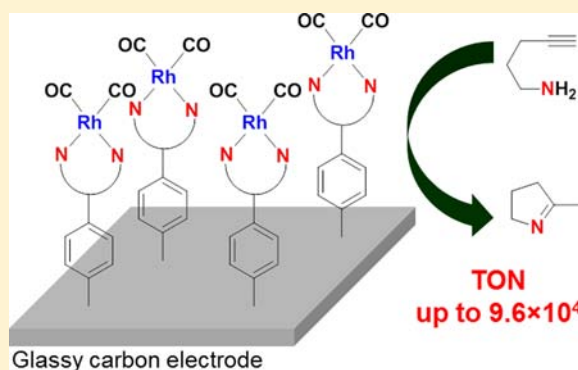
Rh(I) Complexes Bearing *N,N* and *N,P* Ligands Anchored on Glassy Carbon Electrodes: Toward Recyclable Hydroamination Catalysts

Andrey A. Tregubov, Khuong Q. Vuong, Erwann Luais, J. Justin Gooding, and Barbara A. Messerle*

School of Chemistry, The University of New South Wales, Sydney 2052, Australia

S Supporting Information

ABSTRACT: A series of *N,N*-donor ligands (*bis*(pyrazol-1-yl)methane (bpm), *bis*(*N*-methylimidazol-2-yl)methane (bim), 1-(phenylmethyl)-4-(1*H*-pyrazol-1-yl methyl)-1*H*-1,2,3-triazole (PyT)), and one *N,P*-donor ligand precursor (1-(3,5-dimethylpyrazol-1-yl)(2-bromoethane) (dmPyBr)) were synthesized and functionalized with aniline. Diazotization of the aniline into an aryl diazonium, using nitrous acid in aqueous conditions, was performed in situ such that the ligands could be reductively adsorbed onto glassy carbon electrode surfaces. The *N,N*-donor ligands (bpm, bim, PyT) were immobilized in a single step, while several steps were required to immobilize the *N,P*-donor ligand (dmPyP) to prevent oxidation of the phosphine group. The complexation of the anchored ligands with the metal complex precursor ($[\text{Rh}(\text{CO})_2(\mu\text{-Cl})_2]$) led to the formation of anchored Rh(I) complexes with each of the ligands (bpm, bim, PyT, dmPyP). X-ray photoelectron spectroscopy (XPS) confirmed the formation of the anchored ligands as well as the anchored complexes. The surface coverage of functionalized electrodes was estimated by means of cyclic voltammetry, and the nature of the coverage was close to being a monolayer for each immobilized complex. The anchored Rh(I) complexes were active as catalysts for the intramolecular hydroamination of 4-pentyn-1-amine to form 2-methyl-1-pyrroline.



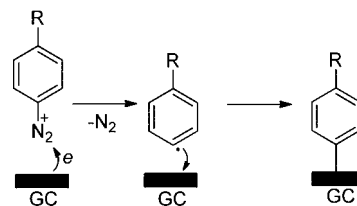
INTRODUCTION

Homogeneous catalysts are readily characterized and optimized leading to highly effective catalysis, while heterogeneous catalysts have the advantage that they are more readily recovered and reused. The immobilization of homogeneous catalysts on solid supports leads to catalysts that take advantage of the best of both homogeneous and heterogeneous catalysis. Ideally, homogeneous catalysts should be immobilized on robust surfaces with robust linkers to give the most effective systems. A wide range of supports have been used for catalyst immobilization, including zeolites,^{1,2} polymers,^{3–5} carbon-based materials,^{6,7} and silica.^{8–13} Of these, silica is the most common support for the immobilization of metal complexes, and although the (Si–O–Si) linkage used for immobilization is quite robust, it can undergo hydrolysis under basic conditions.¹⁴ Several important catalyzed reactions, including the Heck reaction,¹⁵ utilize basic conditions,^{16,17} limiting the breadth of application of silica supported catalysts. Carbon-based materials are useful as catalyst supports as they are typically very stable under harsh conditions including low or high pH and high temperatures. The robust attachment of homogeneous catalysts to inert carbon surfaces is an important challenge, and the use of the stable covalent C–C bond as a linkage between a carbon surface and catalyst ligand is an important approach to catalyst immobilization.

The attachment of a variety of molecules to stable carbon-based surfaces through C–C bonds via the reductive

adsorption of aryl diazonium salts has been widely used for surface functionalization, in particular for biosensor fabrication.^{18–20} Electron donation from the carbon electrode to the aryl diazonium salt results in the formation of a phenyl radical which is then covalently attached to the glassy carbon (GC) surface (Scheme 1).

Scheme 1. Attachment of Molecules to Carbon-Based Surfaces via Reduction of Aryldiazonium Salts



Experimental and theoretical studies^{21,22} confirm that the covalent C–C linkage formed between the surface and aryl layer in this way is very strong, and it has been demonstrated that it is highly resistant toward leaching even under harsh conditions.^{18,19,23} It is therefore rather surprising that there are only limited examples of this approach for immobilizing

Received: June 9, 2013

Published: October 2, 2013

catalysts on carbon surfaces. Stark and Reiser immobilized TEMPO (2,2,6,6-tetramethylpiperidine-1-oxyl)²⁴ and Cu(II)–azabis(oxazoline) complexes²⁵ on graphene-coated cobalt nanoparticles. The immobilized TEMPO catalyst is a highly active catalyst for the oxidation of primary and secondary alcohols and does not lose activity over several catalytic runs. More recently, Geneste et al.²⁶ reported a Cu(II) complex electrochemically immobilized on graphite felt and tested its catecholase activity in continuous flow catalysis. In each of these examples, the catalysis was performed under thermal conditions without any electron transfer from or to the supports. The attachment of molecules to carbon electrodes leading to the formation of effective electrocatalysts using the aryl diazonium method has also been demonstrated. For example, De Lacey et al. attached *Desulfovibrio gigas* hydrogenase to an aniline layer on a glassy carbon electrode,²⁷ and the covalently attached enzyme was active for dihydrogen oxidation via direct electron transfer to the electrode and was significantly more stable than the physisorbed enzyme.

The catalyzed hydroamination reaction is a significant reaction that involves the addition of an N–H bond across an unsaturated C–C bond and is a highly efficient approach to the synthesis of many valuable nitrogen containing compounds (amines, imines, and enamines).²⁸ We have shown previously that Rh(I) and Ir(I) complexes bearing a range of *N,N*-donor and *N,P*-donor ligands are highly effective catalysts for intramolecular hydroamination of alkenamines^{29–32} and alkenamines.^{33,34} Here we report the immobilization of a selection of these catalysts on glassy carbon surfaces. Bidentate pyrazolyl- and imidazolyl-based ligands including *bis*(pyrazol-1-yl)methane (bpm) and *bis*(*N*-methylimidazol-2-yl)methane (bim) and mixed pyrazol-1-yl-1,2,3-triazol-4-ylmethane (PyT) and 1-(3,5-dimethylpyrazol-1-yl)-2-diphenylphosphinoethane (dmPyP) ligands were immobilized on glassy carbon electrodes and the corresponding supported Rh(I) complexes (Figure 1) synthesized. The application of these immobilized complexes as catalysts for the intramolecular hydroamination reaction is demonstrated.

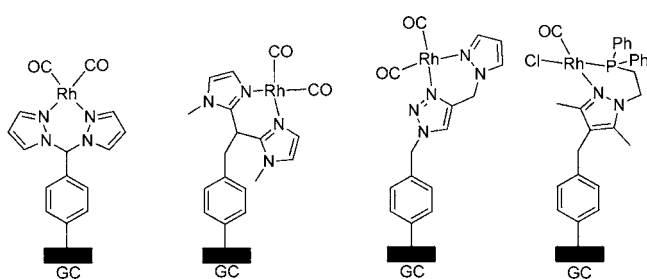


Figure 1. Bidentate Rh(I) complexes with the *N,N* donor ligands (bpm, bim, and PyT) and *N,P* donor ligand (dmPyP) immobilized on a glassy carbon support.

GENERAL EXPERIMENTAL SECTION

Synthesis of Ligands. Three different aniline-functionalized ligands bpm-NH₂, bim-NH₂, and PyT-NH₂ (Figure 2 (1–3)) and one ligand precursor dmPyBr-NH₂·HCl were synthesized (Figure 2 (4)). The procedures for the synthesis of these compounds are provided in the Supporting Information.

Glassy Carbon (GC) Plate Modification. The modifications of GC plate surfaces with the *N,N*-donor ligands (bpm, bim and PyT) and pro-ligand dmPyBr were achieved using the in situ generated aryl diazonium salts of bpm-NH₂ (1), bim-NH₂ (2), PyT-NH₂ (3), and

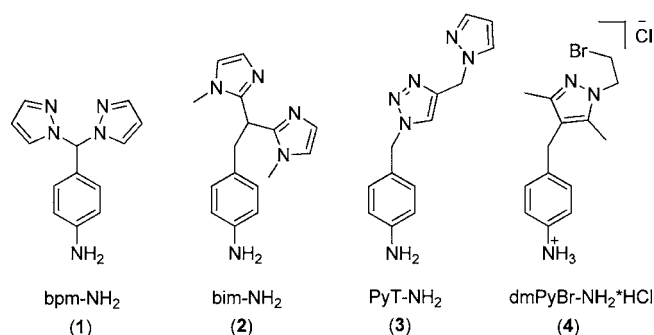


Figure 2. Aniline-functionalized ligands (1–3) and pro-ligand (4).

dmPyBr-NH₂·HCl (4), respectively, in acidic media following reported methods.³⁵ A conventional three-electrode system was set up for the modification of the GC plate (Goodfellow, product code VC000502) using a platinum wire as the counter electrode, an Ag/AgCl 1.0 M KCl electrode as the reference electrode, and finally the GC plate (1 × 1 × 0.1 cm) as the working electrode. All potentials were reported versus the Ag/AgCl reference electrode. The glassy carbon electrodes were polished successively with 1.0, 0.3, and 0.05 μm alumina (Al₂O₃) slurries and Milli-Q water on microcloth pads. The carbon plates were thoroughly rinsed with Milli-Q after polishing and then soaked for 30 min in dichloromethane. Before modification, the electrodes were dried under a nitrogen stream.

Aqueous sodium nitrite (100 mM, 100 μL) was added to a solution of the aniline-functionalized ligands (1, 2, or 3) and pro-ligand (4) (1 mM), and aqueous hydrochloric acid (0.5 M, 10 mL) at 0 °C was added to generate the aryl diazonium salt in the electrochemical cell in situ. The mixture was degassed by bubbling with nitrogen and allowed to react for about 10 min at 0 °C. The electrochemical reduction of the in situ generated diazonium salt was carried out by scanning in a potential range between 0.6 and –1.0 V versus Ag/AgCl for two cycles at the scan rate of 100 mV × s^{–1} leading to the formation of the immobilized ligands GC-bpm, GC-bim, GC-PyT, and GC-PyBr. After this grafting step, the GC plates were rinsed with copious amounts of Milli-Q water, acetonitrile, and ethanol, then dried under a stream of nitrogen.

To prepare the immobilized phosphine–pyrazolyl ligand dmPyP on GC, a stepwise approach was taken. A GC electrode functionalized with the pro-ligand (4) was treated with 1 mL of diphenylphosphide solution (0.1 M, generated by reacting 0.1 g Ph₂PH (0.5 mmol) in 5 mL of tetrahydrofuran (THF) with 0.35 mL of *n*-butyllithium (1.6 M in hexanes) at 0 °C overnight. The solvent was decanted, and the electrode was washed with deoxygenated THF (3 × 2 mL), deoxygenated water (3 × 2 mL), and then with deoxygenated methanol (3 × 2 mL) to afford the immobilized ligand, GC-dmPyP.

Complexation of Immobilized Ligands with Rh(I). The modified electrodes bearing the immobilized ligands (GC-bpm, GC-bim, GC-PyT, and GC-dmPyP) were placed in a THF solution of [Rh(CO)₂(μ-Cl)]₂ (0.5 mM, 2 mL) under an atmosphere of argon for 2 h. After decantation of the solvent, the electrodes were consecutively rinsed three times with THF (5 mL) and methanol (5 mL) and then dried under a stream of nitrogen.

Characterization of the Modified Surfaces. Surface analysis of the modified GC plates was performed using XPS with an EscaLab 250 Xi (Thermo Scientific) spectrometer with a monochromated Al Kα source. The measurements were recorded at a pressure of below 10–8 mbar in the analysis chamber and a takeoff angle normal to the sample surface. The pass energy and the step size for the survey scan was 100 and 1.0 eV, respectively, and 20 and 0.1 eV, respectively, when monitoring narrow scans. The analysis was focused on the center of the modified area to avoid contamination from the edges of the electrodes. Spectral analysis was performed using Avantage 4.73, the background spectra were considered as Shirley type and curve fitting was carried out using a mixture of Gaussian–Lorentzian functions.

Attempts to confirm the presence of Rh-bound CO groups on the surface using surface IR were not successful. This is likely to be due to the fact that the complex layer on the surface is very thin (CV showed the layer to be a monolayer) and that carbon materials strongly absorb light in the UV–vis–IR regions masking IR signals. Carbon surfaces also lack the ability to support electromagnetic field enhancement in surface-enhanced Raman spectroscopy.³⁶

Evaluation of Rh Content on Electrode Surface. The evaluation of Rh content on the electrode surface was accomplished using cyclic voltammetry (potential range from -0.5 and 1.5 V versus Fc/Fc^+) in acetonitrile using $n\text{-Bu}_4\text{NBF}_4$ (1 M) as the supporting electrolyte. The cyclic voltammetry was acquired using an Autolab PGStat12 Potentiostat. The glassy carbon rodlike electrodes (surface area approximately 0.07 cm^2 /each) functionalized with Rh complexes according to methodology described above were used as working electrodes. Platinum wires were used both as the counter electrode and the reference electrode. All potentials were reported versus Fc/Fc^+ couple. The surface coverage (Γ) was evaluated using formula $\Gamma = Q/nFA$, where Q is the charge measured during the oxidation of a surface-bound Rh complex, F is the Faraday constant, n is the number of electrons employed in the electrochemical reaction (for the oxidation Rh(I) to Rh(II) $n = 1$), and A is the surface area of the working electrode.³⁷ The ratio of Rh coverage to surface area obtained for rodlike electrodes was then used to calculate the Rh content for the glassy carbon plates (surface area of one side is 1 cm^2 , the full surface area is 2.4 cm^2 in order to calculate the TON of catalyzed reaction described below).

Catalyzed Hydroamination of 4-Pentyn-1-amine Using Immobilized Complexes. A functionalized electrode was placed in 1.0 mL of anhydrous THF in an amber vial purged with nitrogen. 4-Pentyn-1-amine (0.0200 ± 0.0005 g, 0.024 mmol) was added, the vial was sealed with a Teflon-lined screw-on lid, and the reaction was heated at 60 $^\circ\text{C}$ for 72 h under an inert atmosphere. To optimize the flow of the substrate past the catalyst on the electrode surface, the vial was spun (300 rpm) for the entire reaction time (for a picture of the setup, see Figure S111 in the Supporting Information). The reaction was then cooled to ambient temperature, and the conversion of substrate to product was determined using ^1H NMR spectroscopy. The turnover numbers (TON) was calculated using the following formula:

$$\text{TON} = \frac{[\text{moles of product}]}{[\text{moles of Rh}]}$$

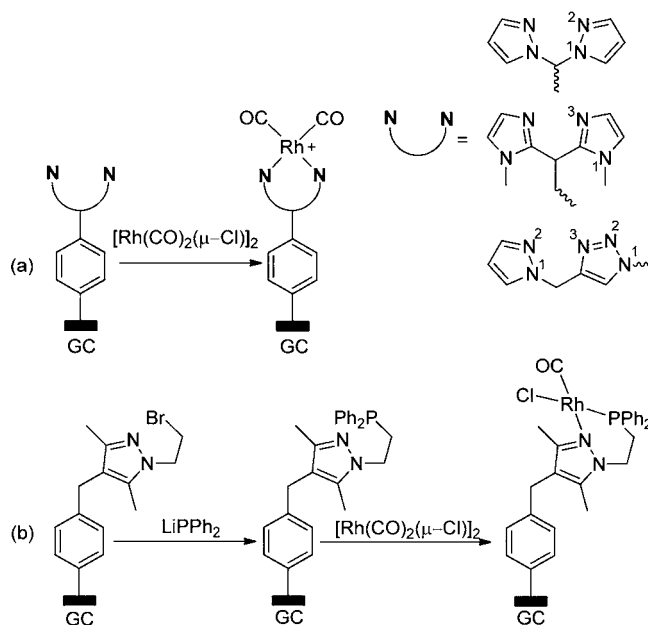
where [moles of product] is the amount of 2-methyl-1-pyrroline measured from ^1H NMR spectra, and [moles of Rh] is the amount of Rh on the electrode surface estimated by cyclic voltammetry.

RESULTS AND DISCUSSION

Synthesis of Aryl Amino-Functionalized Ligands. The immobilization of metal complexes on glassy carbon surfaces via C–C bond described here required the initial functionalization of the N,N -donor ligands and the pro-ligand of the N,P -donor ligands with aniline moieties (Figure 2, (1–4)). The position of the aniline linker varied depending on the symmetry and structure of a ligand. In the case of the bis N,N ligands (bpm and bim) the linker was introduced at the CH_2 bridge between the azole rings (Figure 2 (1 and 2)). The ligand pyrazol-1-yl-1,2,3-triazol-4-ylmethane (PyT) and pro-ligand 1-(3,5-dimethyl-pyrazol-1-yl)-2-bromoethane (dmPyBr) were functionalized with aniline at the N1 position of the 1,2,3-triazolyl and the C4 position of the pyrazolyl ring, respectively (Figure 2, (3 and 4)).

Immobilization of Functionalized Ligands and Preparation of Immobilized Catalysts. The synthesis of the anchored Rh(I) complexes of the N,N ligands (bpm, bim, PyT) was accomplished in two steps (Scheme 2(a)). The functionalized N,N ligands were grafted on the GC electrodes by the

Scheme 2. Synthesis of Anchored Rh(I) Complexes Using Ligands Immobilized According to Scheme 1: (a) N,N -Donor Ligands; (b) N,P Donor Ligand



reductive adsorption of their aryl diazonium salts, which were generated in situ in aqueous conditions using electrochemical assistance as illustrated in Scheme 1. The cyclic voltammogram of the diazonium salt generated from bpm- NH_2 is shown in Figure 3. The first scan contains the broad irreversible peak

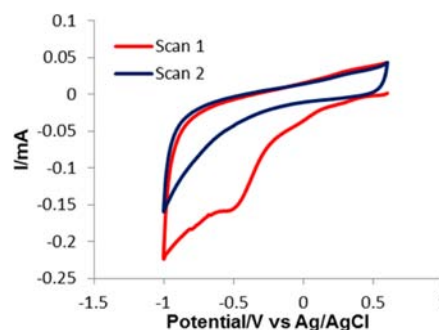


Figure 3. Cyclic voltammogram of diazonium salt bpm- N_2^+ generated from bpm- NH_2 .

attributed to the reduction of the aryl diazonium salt bpm- N_2^+ . The second scan does not have any peaks showing that the electrode surface is fully functionalized with the aryl layer which blocks the electron transfer between the electrode surface and the diazonium salt and confirms the complete surface coverage. The cyclic voltammograms of diazonium salts generated from bim- NH_2 , PyT- NH_2 , and PyBr- $\text{NH}_2 \cdot \text{HCl}$ can be found in the Supporting Information (Figures S11–S13, Supporting Information).

The anchored metal complexes GC- $[\text{Rh}(\text{bpm})(\text{CO})_2]^+$, GC- $[\text{Rh}(\text{bim})(\text{CO})_2]^+$, and GC- $[\text{Rh}(\text{PyT})(\text{CO})_2]^+$ were synthesized by the addition of a solution of $[\text{Rh}(\text{CO})_2(\mu\text{-Cl})_2]$ in THF to the immobilized ligands, in an analogous fashion to the synthesis of the parent homogeneous complexes $[\text{Rh}(N,N)(\text{CO})_2]^+$. The formation of the Rh(I) dicarbonyl complexes was confirmed using XPS (see below); however, the precise

Table 1. XPS Data of Anchored Ligands and Pro-ligand dmPyBr^a

sample	binding energy					atomic ratio		
	N 1s			Br 3d	P 2p	N ^b /N ^c	N/Br	N/P
	N ^a	N ^b	N ^c					
GC-bpm	n/a	401.2	399.7	n/a	n/a	1.1	n/a	n/a
GC-bim	n/a	401.5	399.5	n/a	n/a	1.0	n/a	n/a
GC-PyT	401.9	401.0	399.8	n/a	n/a	1.3	n/a	n/a
GC-dmPyBr	n/a	401.4	399.9	71.4	n/a	1.0	1.7	n/a
GC-dmPyP	n/a	401.5	400.0	n/a	133.0	1.0	n/a	1.9

^aBinding energies are in eV.

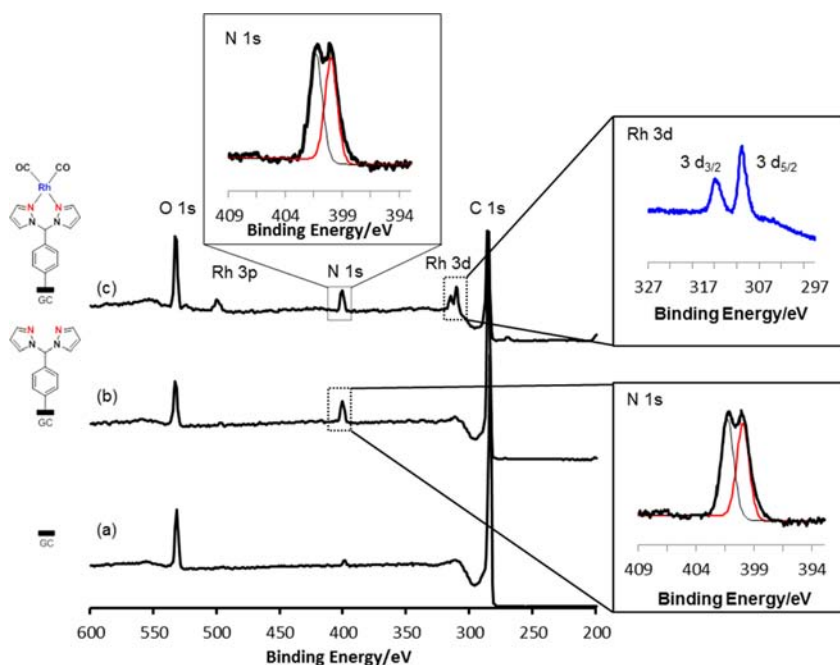


Figure 4. XP spectra: (a) unmodified plate, (b) plate functionalized with bpm, (c) plate (b) after treatment with $[\text{Rh}(\text{CO})_2(\mu\text{-Cl})]_2$.

nature of the counter-anions expected for the positively charged immobilized complexes could not be established. The surface shows the presence of little or no counterion by XPS, indicating that the surface possesses little or no charge. We have also shown previously with XPS of mixed layers containing charged moieties that if the charge is completely neutralized there are no counterions present.³⁸ The unclear nature and location of the counteranion after immobilization of a cationic complex has also been reported by Laws et al.³⁹ Laws et al. immobilized the complex $[\text{CoCp}(\eta^5\text{-C}_3\text{H}_4\text{N}_2)][\text{PF}_6]_2$ on glassy carbon electrodes, and XPS showed only a small amount of fluorine and none of the phosphorus peaks expected for the PF_6 counteranion.

The synthesis of the anchored Rh(I) complex of the *N,P*-donor ligand dmPyP (**4**) was achieved following a modification of the immobilization procedure used for the analogous *N,N*-donor ligands (**1–3**) (Scheme 2(a)). The susceptibility of phosphines to oxidation in the presence of nitrous acid,⁴⁰ which is necessary for diazotization of aniline moiety, makes the direct immobilization of the functionalized *N,P* ligand undesirable, and the addition of the phosphine arm of the ligand was performed after the immobilization of the pro-ligand (**4**) dmPyBr. The aniline hydrochloride-functionalized proligand (**4**) dmPyBr was anchored on the glassy carbon electrode via electrochemical reduction of its aryl diazonium salt (sample GC-dmPyBr) and subsequent treatment of the electrode with a

solution of LiPPh_2 led to the formation of the desired anchored ligand GC-dmPyP (Scheme 2(b)). In contrast to the *N,N* ligands mentioned above, the complexation between the homogeneous counterpart dmPyP ligand and $[\text{Rh}(\text{CO})_2(\mu\text{-Cl})]_2$ results in the formation of a neutral Rh (I) complex $[\text{Rh}(\text{dmPyP})(\text{CO})\text{Cl}]$, with the CO *cis* and Cl *trans* relative to the phosphine donor.⁴¹ The analogous immobilized complex GC- $[\text{Rh}(\text{dmPyP})(\text{CO})\text{Cl}]$ was formed on reaction of the immobilized dmPyP ligand (GC-dmPyP) with a solution of $[\text{Rh}(\text{CO})_2(\mu\text{-Cl})]_2$ (Scheme 2(b)), as confirmed by XPS (below).

X-ray Photoelectron Spectroscopy. X-ray photoelectron spectroscopy (XPS) was used to characterize both the anchored ligands and complexes. XPS data (binding energies and atomic ratios) for the anchored ligands are summarized in Table 1. The XP spectra shown in Figure 4 are for the immobilized ligand GC-bpm and the corresponding immobilized Rh complex, while the analogous spectra for the samples GC-bim, GC-dmPyBr, and GC-dmPyP are included in the Supporting Information. The XP survey spectra of the GC-bpm, GC-bim, GC-dmPyBr, GC-dmPyP plates contain N 1s peaks at ca. 400 eV, which confirms the success of the immobilization of ligands.

The N 1s high resolution spectra of samples GC-bpm, GC-bim, GC-dmPyBr, and GC-dmPyP display two peaks at ca. 401 and 400 eV (Table 1, N^b and N^c, respectively). The peak with

Table 2. XPS Data Obtained for Anchored Complexes (N in the N/Rh Ratio Is the Sum of All N Species Present)^a

sample	binding energy					atomic ratio				
	N 1s			Br 3d	P 2p	Rh 3d	N ^b /N ^c	N/Rh	P/Rh	Cl/Rh
	N ^a	N ^b	N ^c							
GC-[Rh(bpm)(CO) ₂]	n/a	401.4	400.4	n/a	n/a	309.9	1.2	4.1	n/a	n/a
GC-[Rh(bim)(CO) ₂]	n/a	401.8	400.5	n/a	n/a	310.0	0.9	3.8	n/a	n/a
GC-[Rh(PyT)(CO) ₂]	402.1	401.2	400.2	n/a	n/a	310.3	3	5.3	n/a	n/a
GC-[Rh(dmPyP)(CO)Cl]	n/a	401.3	400.5	132.5	198.6	309.7	1.2	1.8	1.1	0.8

^aBinding energies are in eV.

lower binding energy was assigned to the pyridine like nitrogen atom in each case (for GC-bpm, GC-dmPyBr, GC-dmPyP - N^b is N2 of pyrazole; for GC-bim N^b is N3 of imidazole), whereas the one at higher binding energy was assigned to the pyrrole-like nitrogen of each ligand (for GC-bpm, GC-dmPyBr, GC-dmPyP; N^c is N1 of pyrazole; for GC-bim N^c is N1 of imidazole).^{42–45} The atomic percentages ratio for N^b and N^c is very close to the expected ratio of 1:1.

The N 1s region of XP spectrum of the sample GC-PyT was fitted with three peaks assigned to N1 of 1,2,3 triazole (401.9 eV), N2 of pyrazole and N1 of pyrazole (401.0 eV), and N2/N3 of 1,2,3 triazole (399.8 eV).^{46,47}

The XP survey spectrum of the sample GC-dmPyBr (Figure S16(b) in the Supporting Information) comprises the XPS bromine signal at 71.4 eV, and the atomic content of bromine emission correlated well with that expected for nitrogen (N:Br = 2:1). The survey spectrum of the sample GC-dmPyP (Figure S16(c), Supporting Information), which was obtained by the treatment of GC-dmPyBr with LiPPh₂, contained a phosphorus peak at 133.0 eV and no bromine signal, as expected. This result indicates the full substitution of bromide with diphenyl phosphide. The observed ratio of N:P of 1.9:1, was close to the expected ratio of 2:1. The narrow peak for the phosphorus signal indicates the presence of only one type of phosphorus species, with a binding energy specific for phosphines.⁴⁸ The presence of the O 1s peak in all spectra of all of the surface bounds ligands can be explained by contamination of the surface due to physisorption of oxygen molecules and/or native oxidized carbon species of the GC plates containing functional groups such as phenols or carboxylic acids. The success of the complexation of the anchored ligands with the Rh(I) precursor, [Rh(CO)₂(μ-Cl)]₂, was also confirmed using XPS. The binding energies for Rh 3d_{5/2}, N 1s and P 2p and atomic ratios are given in the Table 2. The survey spectra of samples GC-[Rh(bpm)(CO)₂] (Figure 4(c)), GC-[Rh(bim)(CO)₂] (Figure S14(c) in the Supporting Information), GC-[Rh(PyT)(CO)₂] (Figure S15(c), Supporting Information), and GC-[Rh(dmPyP)(CO)Cl] (Figure S1 7(b), Supporting Information) contain the emission of rhodium at ca. 310 eV (Rh 3d_{5/2}). These values of binding energies for Rh 3d indicate the presence of rhodium in +1 oxidation state and its coordination to N and P donor atoms.^{44,49}

The assignment of the N 1s peaks for the anchored complexes GC-[Rh(bpm)(CO)₂], GC-[Rh(bim)(CO)₂], and GC-[Rh(dmPyP)(CO)Cl] is similar to the assignment for the anchored uncomplexed ligands (GC-bpm, GC-bim, and GC-dmPyP, respectively). The peak at higher binding energy was assigned to the pyrrole-like nitrogen of each ligand (for GC-bpm, GC-dmPyBr, GC-dmPyP; N^c is N1 of pyrazole; for GC-bim N^c is N1 of imidazole) whereas the one at lower binding energies was assigned to pyridine-like nitrogen (for

GC-bpm, GC-dmPyBr, GC-dmPyP; N^b is N2 of pyrazole; for GC-bim N^b is N3 of imidazole). The sample GC-[Rh(PyT)(CO)₂] has three different nitrogen emissions assigned to N1 of 1,2,3 triazole (402.1 eV), N3 of 1,2,3-triazole and N1,2 of pyrazole (401.2 eV), and N2 of 1,2,3-triazole (400.2 eV). The ratio of the atomic percentages of the last two nitrogen environments (N^b/N^c in the Table 2) is close to the expected ratio and correlates well with the assignment. The atomic percentage ratios N:Rh for samples GC-[Rh(bpm)(CO)₂] and GC-[Rh(bim)(CO)₂] (4.1 and 3.8, respectively) confirm the stoichiometry of anchored Rh(I) complexes with bis-azole ligands. In case of the sample GC-[Rh(PyT)(CO)₂] the atomic ratio N:Rh is close to 5, which satisfies the expected value for the Rh(I) complex bearing mixed pyrazolyl-triazolyl ligand. The difference of the binding energies of the N 1s level of N^c between the anchored ligands (GC-bpm, GC-bim, GC-PyT, and GC-dmPyP) and those treated with [Rh(CO)₂(μ-Cl)]₂ (GC-[Rh(bpm)(CO)₂], GC-[Rh(bim)(CO)₂], GC-[Rh(PyT)(CO)₂], and GC-[Rh(dmPyP)(CO)Cl]) is ca. 0.5 eV. Figure 5

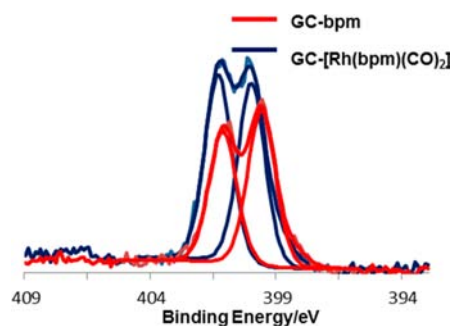


Figure 5. Overlay of the N 1s high-resolution scans of the XP spectra of the samples GC-bpm and GC-[Rh(bpm)(CO)₂].

illustrates the difference of the binding energies of N 1s level between GC-bpm and GC-[Rh(bpm)(CO)₂]. This difference indicates the binding between Rh and N as donor atoms of the ligands

Surface Coverage. The cyclic voltammogram (CV) of the anchored complex GC-[Rh(bpm)(CO)₂] is shown in Figure 6. The irreversible oxidation peak at ca. 0.4 V was assigned to the oxidation of anchored Rh(I) to Rh(II). The second quasi-reversible peak at ca. 0.8 V may be due to the couple Rh(III)/Rh(II). The reversibility of the couple Rh(II)/Rh(I) and Rh(III)/Rh(II) could be ligand-dependent.⁵⁰ In contrast, the cyclic voltammogram of the immobilized ligand bpm does not contain any peaks.

The experimental value of Γ obtained from the integration of the oxidation peak is 6.5×10^{-10} mol/cm². The theoretical value of Γ can be estimated based on the footprint of anchored organometallic complex (see the Supporting Information). The

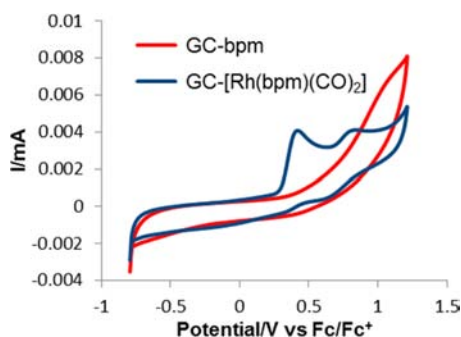


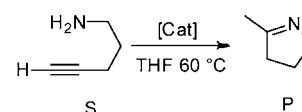
Figure 6. CV using glassy carbon electrodes of GC-bpm and GC-[Rh(bpm)(CO)₂] as working electrodes.

molecular surface of the cationic fragment of complex [Rh(bpm)(CO)₂]BPh₄ was roughly estimated to be ca. 37 Å². Therefore the theoretical value of Γ for such molecule is estimated to be ca. 4.5×10^{-10} mol/cm². The experimental surface coverage obtained from CV is compatible with the presence of a monolayer. Similar surface coverages were obtained for the other complexes under investigation (see Table 3). The experimental values of Γ were used to estimate the amount of Rh on the glassy carbon electrode with an apparent surface area of ca. 2.4 cm² (full available surface area) in order to evaluate the turnover number (TON) in the catalyzed hydroamination of 4-pentyn-1-amine.

Intramolecular Hydroamination of 4-Pentyn-1-amine to 2-Methyl-1-pyrroline Catalyzed by Immobilized Complexes. The catalytic activity of the immobilized complexes GC-[Rh(*N,N*)(CO)₂] and GC-[Rh(*N,P*)(CO)Cl] was investigated using intramolecular hydroamination of 4-pentyn-1-amine as a test reaction (Scheme 3). The cyclization using the immobilized complexes was carried out in sample tubes thoroughly sealed with Teflon tape, with 20 mg of substrate in 1 mL of THF at 60 °C. To achieve effective distribution of the homogeneous substrate in the reaction media the sample tubes were spun for the entire reaction time using a mechanical stirrer (see the Supporting Information). This set up minimizes any mechanical damage of the GC supports on stirring. The results of the catalyzed hydroamination using the immobilized complexes, as well as the efficiency of their homogeneous counterparts, are given in Table 4. The homogeneous catalysis given in the Table 4 was carried out in NMR tubes equipped with Youngs Teflon valve, using the comparable quantity (40 mg) of the substrate used for the catalysis using immobilized complexes, with 1.5 mol % of the corresponding homogeneous Rh complex in deuterated THF solvent at 60 °C.

All immobilized Rh(I) complexes of the *N,N*-donor ligands were active catalysts for the hydroamination of 4-pentyn-1-amine, and 2-methyl-1-pyrroline was the only product observed. The control experiment carried out using a blank (unfunctionalized) electrode did not show any traces of the

Scheme 3. Catalyzed Intramolecular Hydroamination of 4-Pentyn-1-amine



product in the ¹H NMR spectrum. For the immobilized complexes of the *N,N*-donor ligands the conversion of 4-pentyn-1-amine to 2-methyl-1-pyrroline was ca. 50%, and for the immobilized complex with the *N,P*-donor ligand the conversion was significantly reduced (ca. 15%). This mirrored the observations for the analogous homogeneous complexes: the homogeneous complexes based on *N,N*-donor ligands are much faster than those with *N,P*-donor ligands.³⁰ The fact that full conversions of 4-pentyn-1-amine to 2-methyl-1-pyrroline were not achieved with our immobilized catalysts suggests that the catalyst may deactivate during the catalysis process, or that the mass transport effects reduce the interaction of the substrate in solution with the catalyst bound to the surface. If the lack of full conversion is due to catalyst deactivation, the exact nature of the deactivation pathway is not known at this stage, and could be due to product inhibition or clustering of metal centers. Hashmi et al. recently reported extremely reactive mononuclear Au complexes with NHC bound ligands as catalysts for the tandem hydroalkoxylation reaction and made the observation that bulky ligands led to a more stable catalyst, attributing this to the increased in site separation between metal centers which led to lesser extent of catalyst deactivation by clustering of metal centers.⁵¹ Any catalyst deactivation is unlikely to result from the breaking of the very strong C–C bond between the ligand and the surface, as has been reported previously for species attached to carbon surfaces using this approach.^{19,22,23,52} In this work we have shown (see Catalyst Stability) that the ligand remains bound to the surface during the course of a catalytic run.

The TONs for the hydroamination of 4-pentyn-1-amine catalyzed by the immobilized complexes were calculated using the number of moles of product determined from ¹H NMR spectra divided by the number of moles of Rh on the electrode surface estimated using cyclic voltammetry. The calculated TONs for the immobilized complexes are significantly higher (3.7×10^4 – 9.6×10^4) than those of their homogeneous counterparts (Table 4). The two highest turnover frequencies (TOFs) reported in the literature for this particular transformation are attributed to [Me₂Si(η⁵-Me₄C₅)(tBuN)U(NMe₂)₂]⁵³ and [Ir(Me₂PyP)(COD)]BPh₄³² at 1210 and 3100 h⁻¹, respectively, with corresponding TONs of 333 and 71. In the vast majority of homogeneous metal catalyzed hydroamination reactions between 0.5 and 5.0 mol % of catalyst have been used which allows a maximum TON of between 20 and 200 and limits the comparison with the low concentration of the surface immobilized catalysts under investigation here.

Table 3. Experimental and Theoretical Surface Coverage for the GC Supports Modified with Organometallic Complexes (See the Supporting Information for a Calculation Example)

sample	theoretical Γ , mol/cm ²	experimental Γ , mol/cm ²	amt of Rh on 2.4 cm ² glassy carbon electrode, mol
GC-[Rh(bpm)(CO) ₂]	4.5×10^{-10}	5.6×10^{-10}	1.34×10^{-9}
GC-[Rh(bim)(CO) ₂]	4.4×10^{-10}	4.8×10^{-10}	1.15×10^{-9}
GC-[Rh(PyT)(CO) ₂]	3.8×10^{-10}	5.10×10^{-10}	1.22×10^{-9}
GC-[Rh(dmPyP)(CO)Cl]	3.2×10^{-10}	4.0×10^{-10}	0.96×10^{-9}

Table 4. Comparison of the Efficiency of the Catalyzed Cyclization of 4-Pentyn-1-amine to 2-Methyl-1-pyrroline (Scheme 3) Using the Immobilized Catalysts GC-[Rh(*N,N*)(CO)₂] and GC-[Rh(dmPyP)(CO)Cl] and Their Homogeneous Counterparts^a

catalyst	conversion S→P, % (h)		TON	
	complex immobilized on GC electrode ^b	homogeneous complex ^c	complex immobilized on GC electrode ^b	homogeneous complex ^c
[Rh(bpm)(CO) ₂]	50 (72)	90 (12) ⁵⁷	89000	60 ⁵⁷
[Rh(bim)(CO) ₂]	46 (72)	98 (14) ⁵⁷	96000	65 ⁵⁷
[Rh(PyT)(CO) ₂]	49 (72)	70 (5) ³⁴	96000	46 ³⁴
[Rh(dmPyP)(CO)Cl]	15 (72)	72 (45), ^{32, d}	37000	48 ³²

Conditions:

^aConditions: [Rh(*N,N*)(CO)₂]BPh₄ for *N,N* ligands, [Rh(PyP)(CO)Cl] for *N,P* ligand. ^bConditions: 0.24 mmol of the substrate, ca. 5.4×10^{-4} mol % of Rh. ^cConditions: 0.50 mmol of the substrate, 1.5 mol % of Rh. ^dThe analogous complex [Rh(PyP)(CO)Cl] was used.

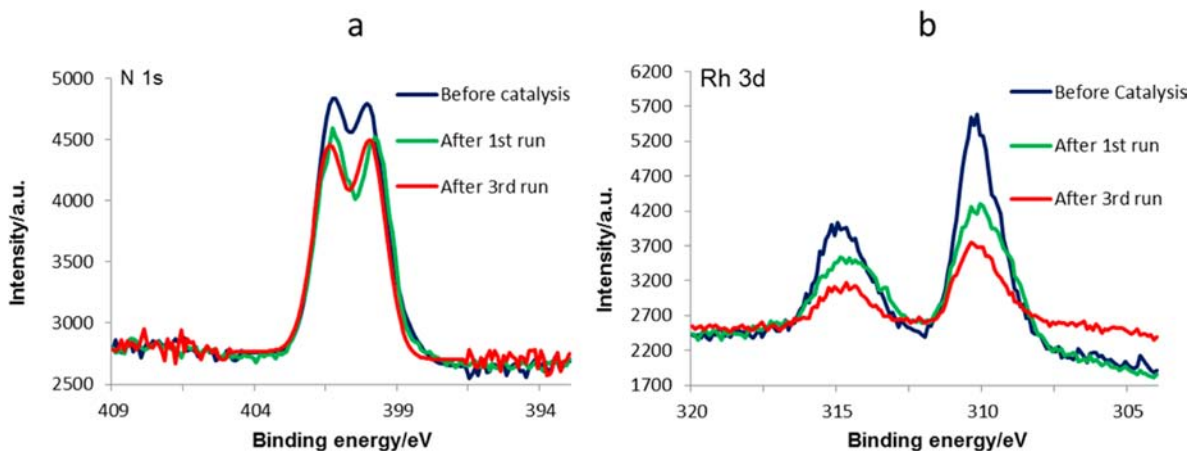


Figure 7. Catalyst recycling: XP spectra of GC-[Rh(bpm)(CO)₂] before and after catalysis: (a) N 1s; (b) Rh 3d.

The hydroamination of 4-pentyn-1-amine catalyzed by heterogeneous catalysts has not previously been reported. However, the catalyzed cyclization of 5-hexyn-1-amine using supported catalysts has been reported. The silica supported Pd complex silica/*cis*-[PdMe(Cl)(PMe₃)₂] can promote the cyclization of 5-hexyn-1-amine with up to 85% conversion after 20 h (0.88 mmol of substrate, 1.2 mol % of Pd) and a calculated TON of 72.⁵⁴ Müller et al. also studied the cyclization of 5-hexyn-1-amine using late transition metal (Zn, Rh, Cu) ion-exchanged BEA zeolites.⁵⁵ The conversions of 5-hexyn-1-amine to cyclized product achieved using these catalysts were 85–100% after 8 h (0.53 mmol % of substrate, 1.0 mol % of metal), and the TON values (80–100) for these catalysts were comparable to those achieved using the silica supported Pd complex in the previous example. In both cases the activity of the heterogeneous supported catalyst was higher than that of a homogeneous counterpart, however, the TONs were relatively low.

The amounts of Rh used in the cyclization of 4-pentyn-1-amine assisted with immobilized Rh complexes in the present work were relatively small (approximately 1.3×10^{-9} mol, or 5.4×10^{-4} mol %) in comparison with Rh loading used for hydroamination catalyzed with homogeneous Rh complexes. This leads to incomplete conversion of the full 20 mg of substrate, but with extremely high TONs. These high levels of catalyst efficiency for the immobilized complexes highlight the potential of the methodology used here for catalyst immobilization. The relatively high TON reported here are consistent with high turnover numbers reported for the surface-bound enzyme glucose oxidase relative to those of the glucose oxidase catalysis in solution.⁵⁶ A higher Rh loading on the

surface may be achieved using carbon materials with higher available surface areas, and this is currently under investigation in our laboratory.

Catalyst Stability. The long-term stability of the immobilized complex GC-[Rh(bpm)(CO)₂] under catalytic conditions was assessed by employing a sample of this complex in three consecutive catalytic runs, and determining the amount of cyclized product formed after each run. The surface composition of the immobilized catalyst was also determined using XPS after the first and third catalytic runs. After the completion of the first and third catalytic runs, the Rh 3d peaks have the same binding energies, which indicates that the Rh oxidation state does not change during catalysis. Following the first catalysis run, the intensity of the Rh 3d peak in the XP spectrum decreased by 24% and conversion to product decreased by 30% (from 23% to 16% conversion), while the intensity of the N 1s peak in the XP spectrum only decreased by 5% (Figure 7). Following the third run, the intensity of the Rh 3d peak decreased by a further 9% and the level of conversion to product decreased by a further 56% to 7%, while the intensity of the N 1s peak did not change significantly (<1%). With a change in N/Rh ratio from 4:1 prior to catalysis to 5.3:1 after the first run, it is clear that the Rh is leaching from the surface during catalysis, although the insignificant changes on the XPS data for N 1s shows that the ligand itself remains bound to the surface and completely intact. These observations are consistent with previously reported work showing that the pyrazolyl ligands are relatively weak metal donors and can decoordinate from Rh in solution.^{57,58} Rh leaching due to N–Rh bond cleavage has also been observed previously from the ([Rh(COD)NH₂(CH₂)₂NH(CH₂)₂Si(OMe)₃]BF₄) complex

which had been immobilized on carbon nanotubes via Si–O–C linkage.⁵⁹ It should be possible to reduce the metal leaching observed for the catalysts under investigation here by using more strongly binding metal donors in the ligands, such as π -heterocyclic carbenes.

CONCLUSIONS

Using the reductive adsorption of aryl diazonium salts we immobilized a series of N,N -donor ligands and an N,P -donor ligand on glassy carbon electrodes. The N,N -donor ligands were immobilized electrochemically in a single step, while the immobilization of the N,P -donor ligand required several steps. The complexation between immobilized ligands and $[\text{Rh}(\text{CO})_2(\mu\text{-Cl})_2]$ leads to anchored Rh(I) complexes of these ligands. The success of ligand immobilization as a monolayer on the GC surface and the stoichiometry of the anchored complexes were confirmed by XPS and also by cyclic voltammetry. Anchored Rh(I) complexes of the N,N -donor ligands were active catalysts for the intramolecular hydroamination of 4-pentyn-1-amine, forming 2-methyl-1-pyrroline, with extremely high TON (up to 9.6×10^4). The immobilized catalysts with the N,N -donor ligand could be recycled, although there was evidence of Rh leaching from the surface. The catalyzed reaction is limited by the relatively small surface area of glassy carbon, and the use of materials with high specific surface area (e.g., porous carbon, carbon nanotubes, graphene) may resolve this issue, and the synthesis of immobilized Rh(I) complexes by means of spontaneous adsorption of aryl diazonium salts on these materials is currently being conducted in our laboratory.

This is the first time that Rh(I) complexes have been anchored onto carbon surfaces via robust C–C bonds. The surface attachment significantly increases the catalytic activity of the Rh(I) complexes, leading to TONs that are orders of magnitude greater than those obtained for the homogeneous counterparts. This work could have significant implications in approaches to the anchoring of homogeneous catalysts on surfaces and lead to improvements in industrial applications of immobilized homogeneous catalysts.

ASSOCIATED CONTENT

Supporting Information

Synthesis of aniline-functionalized N,N ligands and N,P proligand. CV of diazonium salts generated from bim-NH₂, PyT-NH₂, and dmPyBr-NH₂-HCl. XPS of GC-bim, GC-PyT, GC-dmPyBr, GC-dmPyP, and their respective Rh(I) complexes. This material is available free of charge via the Internet at <http://pubs.acs.org>.

AUTHOR INFORMATION

Corresponding Author

b.messerle@unsw.edu.au

Notes

The authors declare no competing financial interest.

ACKNOWLEDGMENTS

We are grateful to Dr. Gavin Edwards for help with developing the methodology for the ligand functionalization and to Dr. Nadim Darwish for discussions of the electrochemistry experiments. We thank Professor Mike George and his group at the University of Nottingham for their help. A.T. thanks the Australian Government for the award of an IPRS (International

Research Postgraduate Scholarship). Financial support from UNSW is gratefully acknowledged. This research was supported under Australian Research Council's Discovery Projects funding scheme (project numbers DP1094564 and DP130101838).

REFERENCES

- (1) Ayala, V.; Corma, A.; Iglesias, M.; Rincon, J. A.; Sanchez, F. J. *Catal.* **2004**, *224*, 170.
- (2) Dominguez, I.; Fornes, V.; Sabater, M. J. *J. Catal.* **2004**, *228*, 92.
- (3) Takeda, K.; Oohara, T.; Shimada, N.; Nambu, H.; Hashimoto, S. *Chem.—Eur. J.* **2011**, *17*, 13992.
- (4) Kollhofer, A.; Plenio, H. *Chem.—Eur. J.* **2003**, *9*, 1416.
- (5) Benaglia, M.; Puglisi, A.; Cozzi, F. *Chem. Rev.* **2003**, *103*, 3401.
- (6) Roman-Martinez, M. C.; Diaz-Aunon, J. A.; De Lecea, C. S. M.; Alper, H. *J. Mol. Catal. A: Chem.* **2004**, *213*, 177.
- (7) Lemus-Yegres, L. J.; Such-Basanez, I.; Roman-Martinez, M. C.; Salinas-Martinez de Lecea, C. *Appl. Catal., A* **2007**, *331*, 26.
- (8) Hamasaka, G.; Kawamorita, S.; Ochida, A.; Akiyama, R.; Hara, K.; Fukuoka, A.; Asakura, K.; Chun, W. J.; Ohmiya, H.; Sawamura, M. *Organometallics* **2008**, *27*, 6495.
- (9) Zhou, W.; Li, Y. M.; He, D. H. *Appl. Catal., A* **2010**, *377*, 114.
- (10) Sahoo, S.; Kumar, P.; Lefebvre, F.; Halligudi, S. B. *J. Mol. Catal. A: Chem.* **2007**, *273*, 102.
- (11) Hu, R. H.; Zha, L. F.; Cai, M. Z. *Catal. Commun.* **2010**, *11*, 563.
- (12) Bourque, S. C.; Maltais, F.; Xiao, W. J.; Tardif, O.; Alper, H.; Arya, P.; Manzer, L. E. *J. Am. Chem. Soc.* **1999**, *121*, 3035.
- (13) Miao, Q. J.; Fang, Z. P.; Cai, G. P. *Catal. Commun.* **2003**, *4*, 637.
- (14) Glasspoole, B. W.; Webb, J. D.; Crudden, C. M. *J. Catal.* **2009**, *265*, 148.
- (15) Heck, R. F.; Nolley, J. P., Jr. *J. Org. Chem.* **1972**, *37*, 2320.
- (16) Miyaura, N.; Suzuki, A. *Chem. Rev. (Washington, D.C.)* **1995**, *95*, 2457.
- (17) Sonogashira, K. *J. Organomet. Chem.* **2002**, *653*, 46.
- (18) Pinson, J.; Podvorica, F. *Chem. Soc. Rev.* **2005**, *34*, 429.
- (19) Gooding, J. J. *Electroanalysis* **2008**, *20*, 573.
- (20) McCreery, R. L. *Chem. Rev.* **2008**, *108*, 2646.
- (21) Jiang, D. E.; Sumpter, B. G.; Dai, S. J. *Phys. Chem. B* **2006**, *110*, 23628.
- (22) Toupin, M.; Belanger, D. *J. Phys. Chem. C* **2007**, *111*, 5394.
- (23) Creager, S. E.; Liu, B.; Mei, H.; DesMarteau, D. *Langmuir* **2006**, *22*, 10747.
- (24) Schatz, A.; Grass, R. N.; Stark, W. J.; Reiser, O. *Chem.—Eur. J.* **2008**, *14*, 8262.
- (25) Schatz, A.; Grass, R. N.; Kainz, Q.; Stark, W. J.; Reiser, O. *Chem. Mater.* **2010**, *22*, 305.
- (26) Marion, R.; Muthusamy, G.; Geneste, F. *J. Catal.* **2012**, *286*, 266.
- (27) Ruediger, O.; Abad, J. M.; Hatchikian, E. C.; Fernandez, V. M.; De Lacey, A. L. *J. Am. Chem. Soc.* **2005**, *127*, 16008.
- (28) Muller, T. E.; Hultsch, K. C.; Yus, M.; Foubelo, F.; Tada, M. *Chem. Rev.* **2008**, *108*, 3795.
- (29) Dabb, S. L.; Ho, J. H. H.; Hodgson, R.; Messerle, B. A.; Wagler, J. *Dalton Trans.* **2009**, 634.
- (30) Burling, S.; Field, L. D.; Messerle, B. A.; Rumble, S. L. *Organometallics* **2007**, *26*, 4335.
- (31) Field, L. D.; Messerle, B. A.; Vuong, K. Q.; Turner, P. *Dalton Trans.* **2009**, 3599.
- (32) Field, L. D.; Messerle, B. A.; Vuong, K. Q.; Turner, P.; Failes, T. *Organometallics* **2007**, *26*, 2058.
- (33) Nguyen, T. O.; Man, B. Y. W.; Hodgson, R.; Messerle, B. A. *Aust. J. Chem.* **2011**, *64*, 741.
- (34) Hua, C.; Vuong, K. Q.; Bhadbhade, M.; Messerle, B. A. *Organometallics* **2012**, *31*, 1790.
- (35) Liu, G. Z.; Chockalingham, M.; Khor, S. M.; Gui, A. L.; Gooding, J. J. *Electroanalysis* **2010**, *22*, 918.
- (36) Anariba, F.; Viswanathan, U.; Bocian, D. F.; McCreery, R. L. *Anal. Chem.* **2006**, *78*, 3104.

- (37) Bard, A. J.; Faulkner, L. R. *Electrochemical Methods: Fundamentals and Applications*; Wiley: New York, 1980.
- (38) Gui, A. L.; Yau, H. M.; Thomas, D. S.; Chockalingam, M.; Harper, J. B.; Gooding, J. J. *Langmuir* **2013**, *29*, 4772.
- (39) Laws, D. R.; Sheats, J.; Rheingold, A. L.; Geiger, W. E. *Langmuir* **2010**, *26*, 15010.
- (40) Bakac, A.; Schouten, M.; Johnson, A.; Song, W. J.; Pestovsky, O.; Szajna-Fuller, E. *Inorg. Chem.* **2009**, *48*, 6979.
- (41) Burling, S.; Field, L. D.; Messerle, B. A.; Khuong, Q. V.; Turner, P. *Dalton Trans.* **2003**, 4181.
- (42) Katrib, A.; Elrayyes, N. R.; Alkharafi, F. M. *J. Electron Spectrosc. Relat. Phenom.* **1983**, *31*, 317.
- (43) Shen, C.; Haryono, M.; Grohmann, A.; Buck, M.; Weidner, T.; Ballav, N.; Zharnikov, M. *Langmuir* **2008**, *24*, 12883.
- (44) Strzelec, K.; Wasikowska, K.; Cypriak, M.; Pospiech, P. *J. Appl. Polym. Sci.* **2012**, *124*, 3538.
- (45) Vasnin, S. V.; Cetrullo, J.; Geanangel, R. A.; Bernal, I. *Inorg. Chem.* **1990**, *29*, 885.
- (46) Ciampi, S.; Boecking, T.; Kilian, K. A.; Harper, J. B.; Gooding, J. J. *Langmuir* **2008**, *24*, 5888.
- (47) James, M.; Ciampi, S.; Darwish, T. A.; Hanley, T. L.; Sylvester, S. O.; Gooding, J. J. *Langmuir* **2011**, *27*, 10753.
- (48) Cai, M. Z.; Sha, J. C.; Xu, Q. H. *J. Mol. Catal. A: Chem.* **2007**, *268*, 82.
- (49) Evans, J.; Hayden, B. E.; Newton, M. A. *Surf. Sci.* **2000**, *462*, 169.
- (50) Feller, M.; Ben-Ari, E.; Gupta, T.; Shimon, L. J. W.; Leitus, G.; Diskin-Posner, Y.; Weiner, L.; Milstein, D. *Inorg. Chem.* **2007**, *46*, 10479.
- (51) Blanco, J. M. C.; Boehling, C. R. N.; Serrano-Becerra, J. M.; Hashmi, A. S. K. *Angew. Chem., Int. Ed.* **2013**, *52*, 7963.
- (52) Allongue, P.; Delamar, M.; Desbat, B.; Fagebaume, O.; Hitmi, R.; Pinson, J.; Saveant, J. M. *J. Am. Chem. Soc.* **1997**, *119*, 201.
- (53) Stubbert, B. D.; Stern, C. L.; Marks, T. J. *Organometallics* **2003**, *22*, 4836.
- (54) Richmond, M. K.; Scott, S. L.; Alper, H. *J. Am. Chem. Soc.* **2001**, *123*, 10521.
- (55) Penzien, J.; Haessner, C.; Jentys, A.; Kohler, K.; Muller, T. E.; Lercher, J. A. *J. Catal.* **2004**, *221*, 302.
- (56) Gooding, J. J.; Erokhin, P.; Hibbert, D. B. *Biosens. Bioelectron.* **2000**, *15*, 229.
- (57) Burling, S.; Field, L. D.; Messerle, B. A.; Turner, P. *Organometallics* **2004**, *23*, 1714.
- (58) Ho, J. H. H.; Wagler, J.; Willis, A. C.; Messerle, B. A. *Dalton Trans.* **2011**, *40*, 11031.
- (59) Lemus-Yegres, L. J.; Perez-Cadenas, M.; Roman-Martinez, M. C.; Salinas-Martinez de Lecea, C. *Microporous Mesoporous Mater.* **2011**, *139*, 164.